Geometry and thermodynamics of smeared Reissner–Nordström black holes in d-dimensional AdS spacetime

Bo-Bing Ye(叶伯兵), Ju-Hua Chen(陈菊华)†, and Yong-Jiu Wang(王永久)

College of Physics and Information Science, Hunan Normal University, Changsha 410081, *China*

(Received 14 March 2017; revised manuscript received 15 May 2017; published online 18 July 2017)

We construct a family of d-dimensional Reissner–Nordström-AdS black holes inspired by noncommutative geometry. The density distribution of the gravitational source is determined by the dimension of space, the minimum length of spacetime l, and other parameters (e.g., n relating to the central matter density). The curvature of the center and some thermodynamic properties of these black holes are investigated. We find that the center of the source is nonsingular for $n \geqslant 0$ (under certain conditions it is also nonsingular for $-2 \leqslant n < 0$), and the properties at the event horizon, including the Hawking temperature, entropy, and heat capacity, are regular for $n > -2$. Due to the presence of l, there is an exponentially small correction to the usual entropy.

Keywords: noncommutative geometry, physics of black holes, thermodynamics

PACS: 02.40.Gh, 04.70.–s, 04.70.Dy **DOI:** 10.1088/1674-1056/26/9/090202

1. Introduction

The noncommutativity of spacetime was originally studied by Snyder.[1] It is currently encoded in the commutator $[x^\mu, x^\nu] = \mathrm{i}\vartheta^{\mu\nu}$, where $\vartheta^{\mu\nu}$ is an anti-symmetric matrix which determines the fundamental cell discretization of spacetime much in the same way as the Planck constant discretizes the phase space. In recent years, the noncommutative geometry inspired black hole, based on the coordinate coherent state formalism,[2,3] has been studied intensively. In such a framework, Nicolini *et al.*[4] pointed out that it is not necessary to change the Einstein tensor part of the field equations, and the noncommutative effects can be implemented acting only on the matter source.[4] Furthermore, the noncommutativity eliminates point-like structures in favor of smeared objects in flat spacetime. The effect of smearing is obtained by replacing the point-like gravitational source with a Gaussian distribution of minimal width $\sqrt{\vartheta}$. For instance, the density of mass M becomes

$$\rho_M(r) = \frac{M}{(4\pi\vartheta)^{3/2}} \mathrm{e}^{-\frac{r^2}{4\vartheta}}. \tag{1}$$

In this framework, Nicolini *et al.* first found a noncommutative-inspired Schwarzschild black hole in four dimensions.[4] Then the black hole was extended to the cases including electric charge,[5] cosmological constant,[6] and extra-spatial dimensions.[7,8] More generally, the charged rotating noncommutative black holes were also derived.[9] Furthermore, many authors have studied the effects of noncommutativity on some properties of a black hole (see Ref. [10]), such as thermodynamics,[11–13] Hawking radiation,[14] and geodesic structure.[15] In the study of the noncommutative Schwarzschild black hole, Nicolini *et al.*[4] pointed out that the usual problems of the terminal phase of black hole evaporation no longer exist due to the noncommutativity. Nozari and Mehdipour investigated the Hawking radiation from a noncommutative Schwarzschild black hole.[14] Larrañaga investigated the geodesic structure and the precession of the perihelion in noncommutative Schwarzschild-AdS spacetime.[15] For the noncommutative Reissner–Nordström (RN) black hole, Mehdipour and Nozari *et al.* investigated the tunneling process of charged massive particles;[16,17] Mehdipour and Keshavarz investigated the entropic force;[18] Bhar *et al.* investigated geodesics, the motion of the test particle, and the scattering of scalar waves.[19] In addition, some authors have also studied the 3-dimensional noncommutative AdS spacetime with charge, angular momentum or not.[20–23]

Park pointed out that the Gaussianity is not always required, and showed that three-dimensional analog of de Sitter black holes does exist when non-Gaussian (ring-type) smearings of point matter hairs are considered.[24] He gave the matter density as

$$\rho_M(r) \sim M\frac{r^n}{L^{n+2}} \mathrm{e}^{-r^2/L^2}, \tag{2}$$

where L is a characteristic length scale of the matter distribution and $n = 0$, 1, 2 correspond to the Gaussian distribution, Rayleigh distribution, and Maxwell–Boltzmann distribution, respectively. The Rayleigh distribution was first introduced by Myung *et al.*[25] In addition, Liang *et al.* investigated thermodynamics of noncommutative 3-dimensional black holes based on the Maxwell–Boltzmann smeared mass distribution.[26] Miao and Xu investigated thermodynamics of noncommutative high-dimensional Schwarzschild–Tangherlini-AdS black holes with this kind of general distribution.[27]

†Corresponding author. E-mail: jhchen@hunnu.edu.cn

© 2017 Chinese Physical Society and IOP Publishing Ltd

The organization of this paper is as follows. In the next section, the wave packet distribution (2) will be extended and a metric solution of the gravitational source with this more general distribution will be given. In Section 3, we study the properties of this metric solution, including the formation of event horizons, curvature of the center, Hawking temperature, entropy, and heat capacity. Finally, a brief conclusion is given.

2. Generalized wave packet distribution and its gravitational field

In this paper, we consider a more general distribution which is an extension of the wave packet distribution (2). Note that for $\mathrm{Re}(k) > 0$, $\mathrm{Re}(d+n) > 0$, and $\mathrm{Re}(1/al^k) > 0$ in d space,

$$\int_0^\infty \omega_{d-1} r^{d-1} \rho(r) \mathrm{d}r = 1 \tag{3}$$

with

$$\rho(r) \equiv \frac{r^n}{\frac{\omega_{d-1}}{k}\Gamma\left(\frac{d+n}{k}\right) a^{\frac{d+n}{k}} l^{d+n}} \mathrm{e}^{-\frac{r^k}{al^k}}, \tag{4}$$

where $\omega_{d-1} = 2\pi^{d/2}/\Gamma(d/2)$ is the area of a unit sphere in $(d-1)$ space. Based on Eq. (3), the densities of total mass M and charge Q can be written as

$$\rho_M(r) = M\rho(r) = M\frac{r^n}{\frac{\omega_{d-1}}{k}\Gamma\left(\frac{d+n}{k}\right) a^{\frac{d+n}{k}} l^{d+n}} \mathrm{e}^{-\frac{r^k}{al^k}}, \tag{5}$$

$$\rho_Q(r) = Q\rho(r) = Q\frac{r^n}{\frac{\omega_{d-1}}{k}\Gamma\left(\frac{d+n}{k}\right) a^{\frac{d+n}{k}} l^{d+n}} \mathrm{e}^{-\frac{r^k}{al^k}}, \tag{6}$$

where n, k, a, and l are all positive, and l is related to the standard deviation or the width of the distribution. For $n > 0$, the density at the center is zero, so the object is hollow. For $n = 0$, the object is solid and regular, and there is an infinite center density for $n < 0$.

The density distribution (5) can be understood from two aspects. One is the noncommutative geometry. If we take $d = 3$, $k = 2$, $a = 1$, and $l = 2\sqrt{\vartheta}$, equation (5) will reduce to Eq. (1); and similarly if we take $d = 2$, $k = 2$, $a = 1$, and $l = L$, equation (5) will reduce to Eq. (2). The other is from quantum mechanics. If there is an object described by wave function $\psi(r)$ with $|\psi(r)|^2 = \rho(r)$, e.g., a bound particle or a Gaussian wave packet, then $\rho(r)$ can be considered as the probability density of the object to be found. An observer will see or think that the mass distribution of the object has a form described by Eq. (5). More specifically, giving $M(r)$ a measured value at point (r, θ, φ), $M(r)$ is then proportional to the probability of finding the object in the region of radius r, i.e.,

$$\frac{M(r)}{M(\infty)} = \frac{\int_0^r \omega_{d-1} r^{d-1} \psi^*(r)\psi(r)\mathrm{d}r}{\int_0^\infty \omega_{d-1} r^{d-1} \psi^*(r)\psi(r)\mathrm{d}r} = \int_0^r \omega_{d-1} r^{d-1} \rho(r)\mathrm{d}r. \tag{7}$$

Since $M(\infty) = M$, equation (7) becomes

$$M(r) = M\int_0^r \omega_{d-1} r^{d-1}\rho(r)\mathrm{d}r = \int_0^r \omega_{d-1} r^{d-1} M\rho(r)\mathrm{d}r. \tag{8}$$

$M\rho(r)$ is therefore equal to $\rho_M(r)$, which is just Eq. (5). In quantum mechanics, l is related to the standard deviation of position, and $l \neq 0$ determined by the uncertainty principle.

The line element describing the spacetime of a static, spherically symmetric distribution of a gravitational field source in $(d+1)$ dimensions has the following form:

$$\mathrm{d}s^2 = -\mathrm{e}^{2\nu(r)}\mathrm{d}t^2 + \mathrm{e}^{2\mu(r)}\mathrm{d}r^2 + r^2\mathrm{d}\Omega_{d-1}^2, \tag{9}$$

where $\mathrm{d}\Omega_{d-1}^2$ is the metric on the unit sphere in $(d-1)$ dimensions and the Einstein–Maxwell field equations read[28]

$$R_{\mu\nu} - \frac{1}{2}Rg_{\mu\nu} + \Lambda g_{\mu\nu} = 8\pi T_{\mu\nu}, \tag{10}$$

$$\frac{1}{\sqrt{-g}}\partial_\mu(\sqrt{-g}F^{\nu\mu}) = \omega_{d-1}J^\nu, \tag{11}$$

with

$$F^{\mu\nu} = (\delta^{0\mu}\delta^{1\nu} - \delta^{0\nu}\delta^{1\mu})E(r), \quad J^\nu = \rho_Q(r)\delta_0^\nu, \tag{12}$$

where $F^{\mu\nu}$ and J^ν are the electromagnetic tensor and the current density, respectively, and the Greek indices μ, ν, ... vary over $0, 1, 2, \ldots, d$.

We take the distribution of the source to be anisotropic and therefore choose the energy–momentum tensor in the form

$$T_{\mu\nu} = (\rho + p_\perp)u_\mu u_\nu + p_\perp g_{\mu\nu} + (p_r - p_\perp)\chi_\mu\chi_\nu + T_{\mu\nu}|_{\mathrm{el}}, \tag{13}$$

where ρ, p_r, $p_\perp$, and $T_{\mu\nu}|_{\mathrm{el}}$ represent the energy density (apart from the electromagnetic field), the radial pressure, the tangential pressure, and the electromagnetic energy–momentum tensor, respectively. u_μ is the velocity of the fluid, and $\chi_\mu = \mathrm{e}^{\mu(r)}\delta_r^\mu$ is an unit vector along the radial direction. Thus, we have

$$T_\nu^\mu = \mathrm{diag}\left(-\rho - \frac{E^2}{2}, p_r - \frac{E^2}{2}, p_\perp + \frac{E^2}{2}, \ldots, p_\perp + \frac{E^2}{2}\right). \tag{14}$$

We do not know the contribution of the charge Q to the energy density ρ, so we take the following form:

$$\rho = \rho_M + \rho_W = (M + W)\rho(r), \tag{15}$$

where W is to be determined.

With the charge density (6), one can solve Eq. (11) to yield

$$E(r) = \frac{Q}{r^{d-1}}\frac{\gamma\left(\frac{d+n}{k}, \frac{r^k}{al^k}\right)}{\Gamma\left(\frac{d+n}{k}\right)}, \tag{16}$$

where $\gamma(s,x)$ is the lower incomplete gamma function

$$\gamma(s,x) \equiv \int_0^x t^{s-1}\,\mathrm{e}^{-t}\,\mathrm{d}t.$$

To preserve the property of RN-AdS metric as $g_{00} = -g_{rr}^{-1}$, we take $p_r = -\rho$. Using the conservation condition $T^{\nu}_{\mu;\nu} = 0$, we can obtain the tangential pressure as

$$p_\perp = -(\rho + E^2) - \frac{r}{d-1}(\rho' + EE'), \tag{17}$$

where the prime represents the derivative with respect to r. For an asymptotic observer,

$$\begin{aligned} M &= \int_0^\infty \omega_{d-1} r^{d-1}(-T_0^0)\,\mathrm{d}r \\ &= M + W + \frac{\pi^{d/2} Q^2 H}{\Gamma\left(\frac{d}{2}\right)\Gamma\left(\frac{d+n}{k}\right)^2}, \end{aligned} \tag{18}$$

so this requires

$$W = -\frac{\pi^{d/2} Q^2 H}{\Gamma\left(\frac{d}{2}\right)\Gamma\left(\frac{d+n}{k}\right)^2}. \tag{19}$$

Then the Einstein–Maxwell field equations lead to the following solution ($d > 2$):

$$\mathrm{d}s^2 = -f(r)\,\mathrm{d}t^2 + f(r)^{-1}\,\mathrm{d}r^2 + r^2\,\mathrm{d}\Omega_{d-1}^2, \tag{20}$$

with

$$\begin{aligned} f(r) &= 1 - \frac{16\pi M}{(d-1)\omega_{d-1}} \frac{1}{r^{d-2}} m(r) \\ &\quad + \frac{8\pi Q^2}{(d-1)(d-2)} \frac{1}{r^{2(d-2)}} q(r) - \frac{2\Lambda r^2}{d(d-1)}, \end{aligned} \tag{21}$$

$$m(r) \equiv \frac{\gamma\left(\frac{d+n}{k}, \frac{r^k}{al^k}\right)}{\Gamma\left(\frac{d+n}{k}\right)}, \tag{22}$$

$$q(r) \equiv \frac{(d-2) r^{d-2}}{\Gamma\left(\frac{d+n}{k}\right)^2}\left[\mathcal{H}(r) + \frac{\gamma\left(\frac{d+n}{k}, \frac{r^k}{al^k}\right)}{\Gamma\left(\frac{d+n}{k}\right)} H\right], \tag{23}$$

$$\mathcal{H}(r) \equiv \int_0^r -x^{1-d}\gamma^2\left(\frac{d+n}{k}, \frac{x^k}{al^k}\right)\mathrm{d}x, \tag{24}$$

and $H = -\mathcal{H}(\infty)$, e.g.,

$$H = \begin{cases} \dfrac{2^{-d}(d+2)\Gamma(d)}{d-2}\left(\dfrac{1}{al}\right)^{d-2}, & \text{for} \quad n = 0, k = 1, \\ 2^{-d/2}\Gamma\left(\dfrac{d-2}{2}\right)\left(\dfrac{1}{al^2}\right)^{\frac{d-2}{2}}, & \text{for} \quad n = 0, k = 2, \\ \dfrac{d}{2(d-2)}\left(2 - 2^{\frac{d-2}{d}}\right)\Gamma\left(\dfrac{d+2}{d}\right)\left(\dfrac{1}{al^d}\right)^{\frac{d-2}{d}}, & \text{for} \quad n = 0, k = d. \end{cases} \tag{25}$$

When $l \to 0$, $m(r) \to 1$, and $q(r) \to 1$ for $n \leqslant 0$, equation (21) reduces to the usual RN-(A)dS metric.[29] For $n > 0$, in order to be reduced to the RN-(A)dS metric, the limit must be taken as $l \to \varepsilon$ with small ε. If we take $l \to 0$ for $n > 0$, both $\rho_M(r)$ and $\rho_Q(r)$ in Eqs. (5) and (6) will be zero, i.e., there will be no gravitational source.

Far away from the center, we can see that the (anti-)de Sitter spacetime is shown in Eq. (21). At the neighborhood of the center, we have

$$\begin{aligned} \frac{\gamma\left(\frac{d+n}{k}, \frac{r^k}{al^k}\right)}{r^{d-2}} &= r^{2+n}\left(\frac{1}{al^k}\right)^{\frac{d+n}{k}}\left[\frac{k}{d+n} + \mathcal{O}(r^k)\right], \\ \frac{\mathcal{H}(r)}{r^{d-2}} &= r^{4+2n}\left(\frac{1}{al^k}\right)^{\frac{2d+2n}{k}} \\ &\quad \times \left[-\frac{k^2}{(d+n)^2(d+2+2n)} + \mathcal{O}(r^k)\right]. \end{aligned} \tag{26}$$

By substituting Eq. (26) into Eq. (21) and retaining only the leading order terms, $f(r)$ becomes

$$\begin{aligned} f(r) &\approx 1 - r^{2+n}\frac{2\Psi_n(k)(al^k)^{-\frac{d+n}{k}}}{(d-1)(d+n)\Gamma(\frac{d+n}{k})^3} - \frac{2\Lambda r^2}{d(d-1)} \\ &\quad - r^{4+2n}\frac{8\pi Q^2 k^2 (al^k)^{-\frac{2d+2n}{k}}}{(d-1)(d+n)^2(d+2n+2)\Gamma\left(\frac{d+n}{k}\right)^2}, \end{aligned} \tag{27}$$

with

$$\begin{aligned} \Psi_n(k) &\equiv 4\pi^{1-\frac{d}{2}} k\Gamma\left(\frac{d}{2}\right)\Gamma\left(\frac{d+n}{k}\right)^2 M - 4\pi k H Q^2 \\ &= 4\pi^{1-\frac{d}{2}} k\Gamma\left(\frac{d}{2}\right)\Gamma\left(\frac{d+n}{k}\right)^2 (M+W), \end{aligned} \tag{28}$$

which shows the (anti-)de Sitter type or just flat for $n \geqslant 0$, depending on the relative values of the parameters Λ, M, Q, l, n, d, a, and k.

3. Properties of the smeared RN-(A)dS black holes

3.1. Formation of event horizons

The horizon radius $r_{\rm h}$ can be found from the equation $g_{00}(r_{\rm h})=0$. In our case we cannot solve analytically $r_{\rm h}$, so we solve M in terms of $r_{\rm h}$, Q, and Λ as

$$M = \frac{(d-1)\omega_{d-1}r_{\rm h}^{d-2}}{16\pi m(r_{\rm h})} \times\left[1+\frac{8\pi Q^2 q(r_{\rm h})}{(d-1)(d-2)r_{\rm h}^{2(d-2)}}-\frac{2\Lambda r_{\rm h}^2}{d(d-1)}\right]. \quad (29)$$

By expanding Eq. (29) near infinity and the center, we can see that

$$M\to\begin{cases}\vartheta(\Lambda)\cdot(-\infty), & \text{for } r_{\rm h}\to+\infty,\\ +\infty, & \text{for } r_{\rm h}\to 0, n>-2,\\ c_1, & \text{for } r_{\rm h}\to 0, n=-2,\\ Q^2\cdot(-\infty), & \text{for } r_{\rm h}\to 0, n<-2,\end{cases} \quad (30)$$

with

$$\vartheta(\Lambda)\equiv\begin{cases}1, & \text{for } \Lambda>0,\\ -1, & \text{for } \Lambda\leqslant 0,\end{cases}$$

where c_1 is finite and larger than zero.

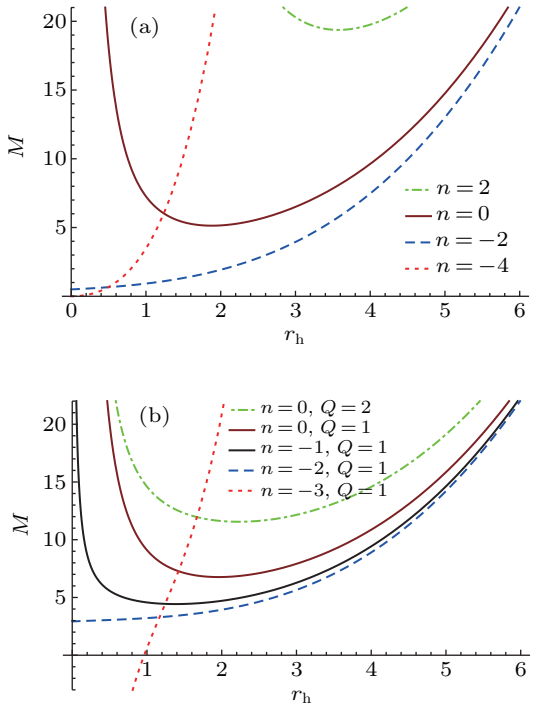


Fig. 1. (color online) Plots of M versus $r_{\rm h}$: (a) $Q=0, \Lambda=-0.5$, and $k=a=l=1$; $d=3$ for $n\geqslant -2$ and $d=5$ for $n<-2$; (b) $\Lambda=-0.5$ and $a=l=1$; $d=3, k=1$ for $n\geqslant -2$ and $d=5, k=2$ for $n<-2$.

The behavior of $M(r_{\rm h})$ is shown in Fig. 1. We can see that when $n>-2$, there are the inner and outer horizons and $M(r_{\rm h})$ has a minimum M_0 at r_0 where the two horizons are merged. For example, $M_0\simeq 2.57l$ and $r_0\simeq 3.38l$ for $Q=\Lambda=n=0$, $k=a=1$, and $d=3$. That means there is an extremal black hole, and no black hole exists with mass less than M_0. In the case of $n\leqslant -2$, there is no extremal black hole. From Fig. 1, we can also find that both M_0 and r_0 increase with the increase of Q and n. More generally, the effects of different parameters on M_0 and r_0 are summarized in Table 1. Table 1 shows that the parameters Q^2, d, n, a, and l have similar effects on M_0 and r_0, while the k parameter is the opposite.

Table 1. The effects of different parameters on M_0 and r_0, e.g., M_0 decreases and r_0 increases with the increase of Λ.

	Q^2	$\Lambda(\leqslant 0)$	d	$n(>-2)$	$k(>0)$	$a(>0)$	$l(>0)$
M_0	+	−	+	+	−	+	+
r_0	+	+	+	+	−	+	+

3.2. Curvature of the center

For the Schwarzschild black hole or RN black hole, we know that there is a gravitational singularity at the center, where the gravitational field becomes infinite in a way that does not depend on the coordinate system. Due to the presence of l, it should be expected that the situation will be different. Curvature invariants of spacetime, e.g., the Kretschmann scalar K ($K\equiv R^{\mu\nu\sigma\tau}R_{\mu\nu\sigma\tau}$), can be used to measure the gravitational field strength and verify the existence of the singularity. Such quantities become infinite within the singularity but finite outside the location, e.g., for the RN black hole, K is infinite for $r=0$ and finite for $r>0$.

The curvature scalar R for the smeared RN-(A)dS metric is found as

$$R = \frac{8\pi Q^2}{(d-1)\Gamma\left(\frac{d+n}{k}\right)^2}\left(2k\,{\rm e}^{-\frac{r^k}{al^k}}(al^k)^{-\frac{d+n}{k}}A_3-(d-3)A_4\right) +\frac{2(d+1)\Lambda}{d-1}+\frac{2\Psi_n(k)(al^k)^{-\frac{d+n}{k}}}{(d-1)\Gamma\left(\frac{d+n}{k}\right)^3} \times\left([(d+1)+n]A_1-\frac{k}{al^k}A_2\right){\rm e}^{-\frac{r^k}{al^k}}, \quad (31)$$

where $R\equiv R^{\mu}_{\mu}$ and

$$A_1\equiv r^n,\quad A_2\equiv r^{n+k},\quad A_3\equiv\frac{\gamma\left(\frac{d+n}{k},\frac{r^k}{al^k}\right)}{r^{d-2-n}},\quad A_4\equiv\frac{\gamma^2\left(\frac{d+n}{k},\frac{r^k}{al^k}\right)}{r^{2(d-1)}}. \quad (32)$$

In addition, the Kretschmann scalar K is given by

$$K = \frac{16}{d^2(d-1)^2\Gamma\left(\frac{d+n}{k}\right)^6}\left\{\frac{1}{2}(d-1)(d-2)\left[\Phi_n(al^k)^{-\frac{d}{k}}+\frac{\Psi_n d}{k}A_5-2q_nA_6\right]^2\right.$$

$$+2(d-1)\left[\Phi_n(al^k)^{-\frac{d}{k}}+\frac{\Psi_n d}{2k}\left[k\mathrm{e}^{-\frac{r^k}{al^k}}(al^k)^{-\frac{d+n}{k}}A_1-(d-2)A_5\right]+q_n[(d-2)A_6+A_4]\right]^2$$
$$+\left[\Phi_n(al^k)^{-\frac{d}{k}}+\frac{\Psi_n d}{2k}\left(-k\mathrm{e}^{-\frac{r^k}{al^k}}(al^k)^{-\frac{d+n}{k}}[(d-3-n)A_1+\frac{k}{al^k}A_2]+(d-1)(d-2)A_5\right)\right.$$
$$\left.-q_n[(d-1)(d-2)A_6-2k\mathrm{e}^{-\frac{r^k}{al^k}}(al^k)^{-\frac{d+n}{k}}A_3+(3d-5)A_4]\right]^2\Big\}, \tag{33}$$

where

$$q_n\equiv 2d\pi Q^2\Gamma\left(\frac{d+n}{k}\right),\quad \Phi_n\equiv\Lambda\Gamma\left(\frac{d+n}{k}\right)^3(al^k)^{\frac{d}{k}},\quad A_5\equiv\frac{\gamma\left(\frac{d+n}{k},\frac{r^k}{al^k}\right)}{r^d}=\frac{A_3}{r^{2+n}},\quad A_6\equiv\frac{\mathcal{H}(r)}{r^d}. \tag{34}$$

At the neighborhood of the center, we obtain

$$\gamma\left(\frac{d+n}{k},\frac{r^k}{al^k}\right)=r^{d+n}\left[\sum_{i=0}^{2}(-1)^i\frac{(al^k)^{-\frac{d+n}{k}}}{\Gamma(i+1)\left(i+\frac{d+n}{k}\right)}\left(\frac{r^k}{al^k}\right)^i+\mathcal{O}(r^{3k})\right],$$

$$\mathcal{H}(r)=r^{d+2n+2}\left[\sum_{j=0}^{2}\sum_{i=0}^{\lfloor\frac{j}{2}\rfloor}\frac{(-1)^{j+1}(\mathrm{sgn}(j-2i)+1)k^2(al^k)^{-\frac{2d+2n}{k}}}{\Gamma(j-i+1)(d+ik+n)[d+(j-i)k+n](d+jk+2n+2)}\left(\frac{r^k}{al^k}\right)^j+\mathcal{O}(r^{3k})\right]. \tag{35}$$

For $n>0$, with $R(0)\equiv\lim_{r\to0}R$ and $K(0)\equiv\lim_{r\to0}K$, one can obtain from Eqs. (31), (33), and (35) that

$$K(0)=\frac{8(d+1)\Lambda^2}{d(d-1)^2}=\frac{2}{d(d+1)}[R(0)]^2,\quad \text{for } n>0. \tag{36}$$

Furthermore,

$$K(0)=\frac{8(d+1)(\Psi_0+\Phi_0)^2}{d(d-1)^2\Gamma\left(\frac{d}{k}\right)^6(al^k)^{\frac{2d}{k}}}=\frac{2}{d(d+1)}[R(0)]^2,\quad \text{for } n=0. \tag{37}$$

Equations (36) and (37) show that there is a simple relationship between K and R at $r=0$ for the smeared RN-(A)dS black hole, but not for the usual black hole. For $n<0$, we will see that R and K are still limited under conditions of Eqs. (38) and (39), even though the central matter density is divergent. For instance, in the case of $-1\leqslant n<0$, in order to avoid the divergent term r^{2n} (or the term A_5) in K, the coefficient of r^{2n} must be zero, i.e., $\Psi_n(k)=0$. More generally, we have

$$K(0)\neq\infty\Leftrightarrow\begin{cases}\Psi_n(k)=0, & \text{for } -1\leqslant n<0,\\ M=Q=0, & \text{for } -2<n<-1,\\ M=Q=0, & \text{for } n<-2,\end{cases} \tag{38}$$

and

$$K(0)\neq\infty\Leftrightarrow\begin{cases}M=Q=0, & \text{for } n=-2,0<k<1,\\ d=3 \text{ and } M-2(\ln4-1)\pi\dfrac{Q^2}{al}=0, & \text{for } n=-2,k=1,\\ M=Q=0, & \text{for } n=-2,1<k<2,\\ \dfrac{4\pi Q^2k^2}{(d-2)^2}+\dfrac{\Psi_{-2}(k)(al^k)^{\frac{d-2}{k}}}{\Gamma\left(\frac{d-2}{k}\right)}=0, & \text{for } n=-2,k\geqslant2.\end{cases} \tag{39}$$

It is interesting to note that in the case of $n=-2$ and $k=1$, the massive object only in $(3+1)$ dimensions is nonsingular. From the above equations, we can see that in the case of $n<0$, the conditions are required to make the curvature limited, but it is not for the case of $n\geqslant0$, which shows that the wave packet with $n\geqslant0$ is always regular.

For a special class of objects with $\Psi_n(k)=0$ (or $\rho=0$, $M=-W$), e.g.,

$$\begin{cases}\pi^{-\frac{d}{2}}\Gamma(\frac{d}{2})\Gamma(d)M-\dfrac{2^{-d}(d+2)}{(al)^{d-2}(d-2)}Q^2=0, & \text{for } n=0,k=1,\\ \pi^{-\frac{d}{2}}\Gamma(\frac{d}{2})^2M-\dfrac{1}{(2al^2)^{\frac{d-2}{2}}(d-2)}Q^2=0, & \text{for } n=0,k=2,\\ \pi^{-\frac{d}{2}}\Gamma(\frac{d}{2})M-\dfrac{2-2^{\frac{d-2}{d}}}{(al^d)^{\frac{d-2}{d}}(d-2)}\Gamma\left(\frac{2}{d}\right)Q^2=0, & \text{for } n=0,k=d,\end{cases} \tag{40}$$

the energy–momentum tensor is equivalent to purely electrical that can be written as

$$T_v^{\mu} = \mathrm{diag}\left(-\frac{E^2}{2}, -\frac{E^2}{2}, -\frac{E^2}{2}+\mathcal{E}, \ldots, -\frac{E^2}{2}+\mathcal{E}\right) \quad (41)$$

with $\mathcal{E} = -rEE'/(d-1)$, and for $n \geqslant -1$ the center is nonsingular. Moreover, $K(0) = 8(d+1)\Lambda^2/d(d-1)^2$ for $n > -1$, which shows that the center is the (anti-)de Sitter type or just flat.

3.3. Hawking temperature and entropy

The Hawking temperature can be calculated as follows:

$$T_{\mathrm{H}} \equiv \frac{\kappa}{2\pi} = \frac{1}{4\pi}\left(\frac{\partial f(r)}{\partial r}\right)_{r=r_+}. \quad (42)$$

By simplifying the above equation for the metric (21), we obtain

$$\begin{aligned} T_{\mathrm{H}} = & \frac{1}{4\pi r_+}\left[(d-2) - \frac{\widehat{g}}{\widehat{m}}\right] \\ & - \frac{2Q^2}{(d-1)r_+^{2d-3}}\left[\widehat{m}^2 + \frac{\widehat{q}}{(d-2)\widehat{m}}\widehat{g} - \frac{Hr_+^{d-2}}{\Gamma\left(\frac{d+n}{k}\right)^2}\widehat{g}\right] \\ & - \frac{\Lambda r_+}{2\pi(d-1)}\left(1 - \frac{\widehat{g}}{d\widehat{m}}\right), \end{aligned} \quad (43)$$

where $\widehat{m} \equiv m(r_+)$, $\widehat{q} \equiv q(r_+)$ and

$$\widehat{g} \equiv g(r_+) = \frac{k\mathrm{e}^{-\frac{r_+^k}{al^k}} r_+^{d+n}}{\Gamma\left(\frac{d+n}{k}\right)(al^k)^{\frac{d+n}{k}}}. \quad (44)$$

In the limit of $l \to 0$, $\widehat{m}$, $\widehat{q}$, and $\widehat{g}$ will be 1, 1, and 0 for fixed r_+. Equation (43) then will be reduced to the Hawking temperature of the RN-(A)dS black hole

$$4\pi T_{\mathrm{H}}(l \to 0) = \frac{d-2}{r_+} - \frac{8\pi Q^2}{(d-1)r_+^{2d-3}} - \frac{2\Lambda r_+}{d-1}. \quad (45)$$

Near infinity or the center, one can find from Eq. (43) that

$$T_{\mathrm{H}} \to \begin{cases} \Lambda\cdot(-\infty), & \text{for} \quad r_+ \to +\infty, \\ -\infty, & \text{for} \quad r_+ \to 0, n > -2, \\ c_2, & \text{for} \quad r_+ \to 0, n = -2, \\ +\infty, & \text{for} \quad r_+ \to 0, n < -2, \end{cases} \quad (46)$$

where c_2 is finite and $c_2 \geqslant 0$.

The Hawking temperature variation is plotted against the black hole radius r_+ in Fig. 2. (i) When $n < -2$, figure 2(a) shows that $T_{\mathrm{H}}(0)$ is divergent, just like the Schwarzschild black hole or RN black hole. (ii) When $n = -2$, T_{H} is positive and finite as r_+ tends to zero. (iii) When $n > -2$, we can see that the temperature is negative where $r_+ < r_0$ (see also Fig. 5), which is not physical; for $r_+ = r_0$ (corresponding to the radius of the extremal black hole), $T_{\mathrm{H}} = 0$ which means a frozen extremal black hole; for $r_+ > r_0$, there is a (local) maximum $T_{\max}$ (where we call $r_{\max}$) to replace the divergence, e.g., $T_{\max} \simeq 0.01/l$ and $r_{\max} \simeq 6.54l$ for $Q = \Lambda = n = 0$, $k = a = 1$, and $d = 3$. Moreover, for $\Lambda = 0$, T_{H} approaches zero as $r_+ \to \infty$. We can also see from Fig. 2(b) that there is a local minimum $T_{\min}$ (where we call $r_{\min}$) when Λ is larger than a critical value and less than zero.

On the other hand, we can find from Fig. 2(a) that, both $r_{\max}$ and r_0 (see also Fig. 1 or Table 1) increase but $T_{\max}$ decreases with the increase of n. More generally, the effects of different parameters on $T_{\max}$, $r_{\max}$, $T_{\min}$, and $r_{\min}$ are shown in Table 2. From Table 2 we can see that the parameters Q^2, n, a, and l have similar effects on $T_{\max}$, $r_{\max}$, $T_{\min}$, and $r_{\min}$, and the k parameter is the opposite. Furthermore, for each parameter, $T_{\max}$ and $T_{\min}$ are affected in the same direction, and from Fig. 2(b) we know that there will be no local maximum and minimum temperature if Λ is too small.

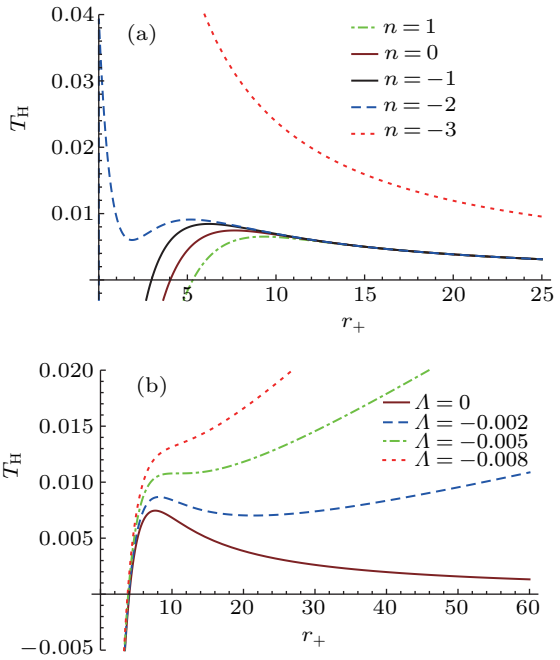


Fig. 2. (color online) Plots of T_{H} versus r_+: (a) $\Lambda = 0$, $Q = 1$, and $a = l = 1$; $d = 3, k = 1$ for $n \geqslant -2$ and $d = 5$, $k = 2$ for $n < -2$; (b) $Q = 1$, $d = 3$, $n = 0$, and $k = a = l = 1$.

Table 2. The effects of different parameters on $T_{\max}$, $r_{\max}$, $T_{\min}$, and $r_{\min}$, e.g., $T_{\max}$ decreases and $r_{\max}$ increases with the increase of Q^2. There is a local minimum $T_{\min}$ only when Λ is larger than a critical value and less than zero.

	Q^2	$\Lambda(\leqslant 0)$	d	$n(>-2)$	$k(>0)$	$a(>0)$	$l(>0)$
$T_{\max}$	−	−	+	−	+	−	−
$r_{\max}$	+	−	+	+	−	+	+
$T_{\min}$	−	−	+	−	+	−	−
$r_{\min}$	−	+	+	−	+	−	−

For the case of charged black hole, the first law of thermodynamics is described by

$$\delta M = \frac{\kappa}{2\pi}\delta S + \Phi\delta Q, \quad (47)$$

where κ, S, and Φ are the surface gravity, entropy, and electric potential on the exterior horizon, respectively. Substituting Eq. (42) into Eq. (47) for fixed electric charge Q, one can derive

$$\mathrm{d}S = \frac{1}{T_{\mathrm{H}}}\mathrm{d}M = 4\pi\left(\frac{\partial g_{00}}{\partial M}\right)^{-1}_{r=r_+}\mathrm{d}r_+. \tag{48}$$

Using Eq. (21), we can obtain

$$\begin{aligned} S &= \int_{r_0}^{r_+}\frac{(d-1)\omega_{d-1}r^{d-2}}{4m(r)}\mathrm{d}r \\ &= \int_{r_0}^{r_+}\frac{(d-1)\Gamma\left(\frac{d+n}{k}\right)\omega_{d-1}r^{d-2}}{4\gamma\left(\frac{d+n}{k},\frac{r^k}{al^k}\right)}\mathrm{d}r. \end{aligned} \tag{49}$$

It is worth noting that the lower limit r_0 of the integral is not equal to zero, and for different parameter values (such as the charge Q), the value of r_0 is different. The behavior of the entropy S with respect to r_+ is shown in Fig. 3. We can see that d, n, and k affect not only the size of r_0, but also the ratio of S to r_+.

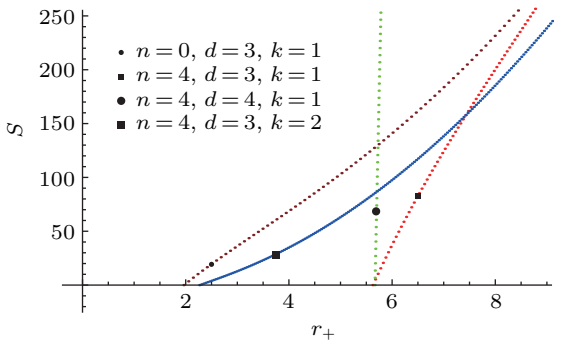


Fig. 3. (color online) Plots of the entropy S versus r_+ for $\Lambda=-0.5$ and $Q=a=l=1$.

By expanding Eq. (49), we can obtain

$$\begin{aligned} S &= \int_{r_0}^{r_+}\frac{(d-1)}{4}\omega_{d-1}r^{d-2} \\ &\quad\times\left(1+\sum_{i=1}^{\infty}\left[\frac{1}{\Gamma\left(\frac{d+n}{k}\right)}\Gamma\left(\frac{d+n}{k},\frac{r^k}{al^k}\right)\right]^i\right)\mathrm{d}r \\ &= \frac{1}{4}\omega_{d-1}r^{d-1}\Big|_{r_0}^{r_+}+\int_{r_0}^{r_+}\frac{(d-1)}{4}\omega_{d-1}r^{d-2} \\ &\quad\times\sum_{i=1}^{\infty}\left[\frac{1}{\Gamma\left(\frac{d+n}{k}\right)}\Gamma\left(\frac{d+n}{k},\frac{r^k}{al^k}\right)\right]^i\mathrm{d}r \\ &\equiv S(r)\big|_{r_0}^{r_+}, \end{aligned} \tag{50}$$

where $\Gamma(s,x)$ is the upper incomplete gamma function

$$\Gamma(s,x)\equiv\int_x^{\infty}t^{s-1}\mathrm{e}^{-t}\mathrm{d}t=\Gamma(s)-\gamma(s,x).$$

From Eq. (50), we can see that the first term is the usual semi-classical Bekenstein–Hawking area law, and the other is the correction to the area law. Expanding $S(r)$ for small l or large r to the leading order, we have

$$\begin{aligned} S(r) &\simeq \frac{1}{4}\omega_{d-1}r^{d-1} \\ &\quad\times\left(1-\sum_{i=1}^{\infty}\frac{d-1}{ik}\left[\frac{\mathrm{e}^{-\frac{r^k}{al^k}}\left(\frac{r^k}{al^k}\right)^{\frac{d+n}{k}-\frac{1}{i}-1}}{\Gamma\left(\frac{d+n}{k}\right)}\right]^i\right). \end{aligned} \tag{51}$$

Hence, one can find that it is an exponentially small correction to the usual entropy due to the fundamental minimum length l.

The heat capacity at a constant charge is given by

$$C\equiv\frac{\partial M}{\partial T_{\mathrm{H}}}=\frac{\partial M}{\partial r_+}\left(\frac{\partial T_{\mathrm{H}}}{\partial r_+}\right)^{-1}=T_{\mathrm{H}}\frac{\partial S}{\partial r_+}\left(\frac{\partial T_{\mathrm{H}}}{\partial r_+}\right)^{-1}, \tag{52}$$

which determines the thermodynamic stability of the black holes. We can see from Fig. 1 and Eq. (30) that $\partial M/\partial r_+$ is generally positive ($\partial M/\partial r_+=0$ at $r_+=r_0$) for $\Lambda\leqslant 0$, so the sign of C is the same as that of $\partial T_{\mathrm{H}}/\partial r_+$. Therefore, the black hole is unstable when $\partial T_{\mathrm{H}}/\partial r_+<0$.

Using Eqs. (43) and (49), we obtain

$$C=\frac{(d-1)\omega_{d-1}}{4\widehat{m}}T_{\mathrm{H}}\left(\frac{\partial T_{\mathrm{H}}}{\partial r_+}\right)^{-1}r_+^{d-2}, \tag{53}$$

with

$$\begin{aligned} \frac{\partial T_{\mathrm{H}}}{\partial r_+} &= -\frac{1}{4\pi r_+^2}\left[(d-2)+\left(d+n-k\frac{r_+^k}{al^k}-1\right)\frac{\widehat{g}}{\widehat{m}}-\frac{\widehat{g}^2}{\widehat{m}^2}\right] \\ &\quad+\frac{2Q^2}{(d-1)r_+^{2d-2}}\left((2d-3)\widehat{m}^2-\widehat{g}\widehat{m}+\widehat{g}\right. \\ &\quad\times\left[\frac{\widehat{g}}{\widehat{m}}-\left(n-k\frac{r_+^k}{al^k}+1\right)\right] \\ &\quad\times\left.\left[\frac{\widehat{q}}{(d-2)\widehat{m}}-\frac{Hr_+^{d-2}}{\Gamma\left(\frac{d+n}{k}\right)^2}\right]\right)-\frac{\Lambda}{2\pi(d-1)d} \\ &\quad\times\left[d-\left(d+n-k\frac{r_+^k}{al^k}+1\right)\frac{\widehat{g}}{\widehat{m}}+\frac{\widehat{g}^2}{\widehat{m}^2}\right]. \end{aligned} \tag{54}$$

The behavior of C is shown in Fig. 4. Figure 4(a) shows the case of $\Lambda=0$. (i) When $n<-2$, $C<0$ (for all r_+), so this black hole is unstable, just like the usual Schwarzschild black hole or RN black hole. (ii) When $n=-2$, the middle black hole is stable and the two sides are unstable. (iii) When $n>-2$, the black hole is stable if $r_0\leqslant r_+<r_{\max}$. When $n>-2$, we see from Fig. 4(b) that Λ has a significant influence on C. $\Lambda=\Lambda_{\mathrm{crit}}$ is a critical case where $T_{\max}=T_{\min}$. (i) When $\Lambda_{\mathrm{crit}}<\Lambda<0$, the black hole is stable for $r_0\leqslant r_+<r_{\max}$ or $r_+>r_{\min}$ (see Fig. 5). C is divergent at $r_{\max}$ or $r_{\min}$ for $\Lambda_{\mathrm{crit}}\leqslant\Lambda<0$, where a phase transition occurs. (ii) When $\Lambda\leqslant\Lambda_{\mathrm{crit}}$, the black hole is stable for all r_+.

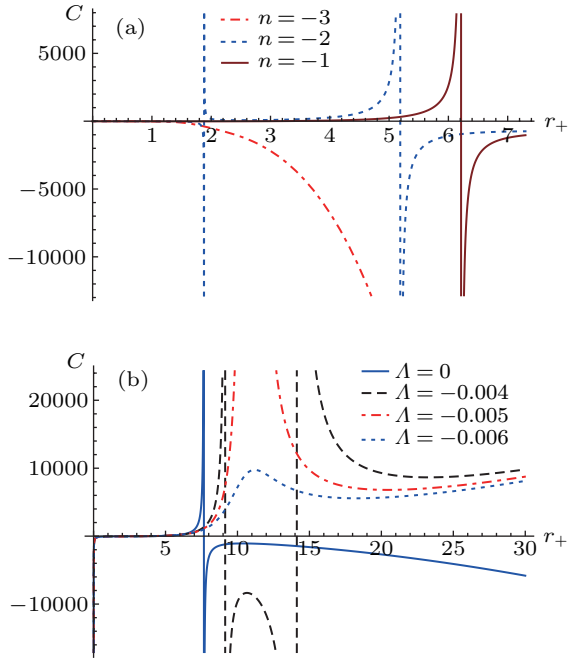


Fig. 4. (color online) Plots of C versus r_+: (a) $\Lambda = 0, Q = 1$, and $a = l = 1$; $d = 3, k = 1$ for $n \geqslant -2$ and $d = 5, k = 2$ for $n < -2$; (b) $Q = 1, d = 3, n = 0$, and $k = a = l = 1$.

Figure 5 shows the behavior of M, $T_{\rm H}$, S, and C for a smeared and regular RN-AdS black hole as a whole. We can see that for a black hole with suitable parameters Q, Λ, d, n, k, a, and l, there is an extremal black hole with $r_+ = r_- = r_0$. The extremal black hole has the minimum total mass, and both its temperature and entropy are equal to zero. In addition, the extremal black hole is also stable. From Table 1 and Table 2, we can find that the parameters Q^2, n, a, and l have similar effects on M (and $T_{\rm H}$), while the k parameter is the opposite to the previous parameters. We can also find that for a higher dimension d, both M and $T_{\rm H}$ will increase for fixed r_+, and the radius of the extremal black hole r_0 will also be greater.

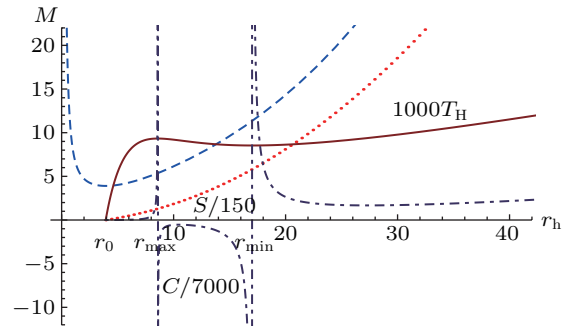


Fig. 5. (color online) Plots of M, $T_{\rm H}$, S, and C as a whole in the case of $Q = 1, \Lambda = -0.003, d = 3, n = 0$, and $k = a = l = 1$.

4. Conclusion

We have constructed a general Reissner–Nordström-(A)dS black hole inspired by noncommutative geometry for which the gravitational source is described by the density distribution (5) and (6), and the characteristics of the spacetime are affected by the following parameters: the total mass M, electric charge Q, cosmological constant Λ, and several parameters affecting the density distribution, including d (the dimension of space), n (relating to the central matter density), l (the minimum length), and so on. This black hole spacetime is asymptotically flat or (A)dS at large distance, and it is flat or the (A)dS type near the center of the gravitational source for $n \geqslant 0$, which depends on the relative values of the above parameters.

By analyzing the central curvature K, the formation of event horizons $r_{\rm h}$, Hawking temperature $T_{\rm H}$, entropy S, and heat capacity C, we found that the center of the source is nonsingular for $n \geqslant 0$, and under certain conditions (describing by Eqs. (38) and (39)) it is also nonsingular for $-2 \leqslant n < 0$. We also found that the Hawking temperature $T_{\rm H}$ has no usual divergence problem for $n > -2$. These results show that about nonsingularity, the critical point of n for the central curvature and thermodynamic properties is different. We have also found that the parameters Q^2, n, a, and l have similar effects on both M and $T_{\rm H}$, while the k parameter is the opposite to the previous parameters. If Λ is too small, there will be no local maximum and minimum temperature. Λ also has an important effect on C. Due to the fundamental minimum length l, there is a correction to the usual semi-classical area law and the correction of entropy decreases exponentially.

References

[1] Snyder H S 1947 *Phys. Rev.* **71** 38
[2] Smailagic A and Spallucci E 2003 *J. Phys. A* **36** L467
[3] Smailagic A and Spallucci E 2003 *J. Phys. A* **36** L517
[4] Nicolini P, Smailagic A and Spallucci E 2006 *Phys. Lett. B* **632** 547
[5] Ansoldi S, Nicolini P, Smailagic A and Spallucci E 2007 *Phys. Lett. B* **645** 261
[6] Nicolini P and Torrieri G 2011 *J. High Energy Phys.* **08** 097
[7] Spallucci E, Smailagic A and Nicolini P 2009 *Phys. Lett. B* **670** 449
[8] Nozari K and Mehdipour S H 2010 *Commun. Theor. Phys.* **53** 503
[9] Modesto L and Nicolini P 2010 *Phys. Rev. D* **82** 104035
[10] Nicolini P 2009 *Int. J. Mod. Phys. A* **24** 1229
[11] Myung Y S, Kim Y W and Park Y J 2007 *J. High Energy Phys.* **02** 012
[12] Banerjee R, Majhi B R and Samanta S 2008 *Phys. Rev. D* **77** 124035
[13] Kim W, Son E J and Yoon M 2008 *J. High Energy Phys.* **04** 042
[14] Nozari K and Mehdipour S H 2008 *Classical and Quantum Gravity* **25** 175015
[15] Larrañaga A 2013 *Rom. J. Phys.* **58** 50
[16] Mehdipour S H 2010 *Int. J. Mod. Phys. A* **25** 5543
[17] Nozari K and Islamzadeh S 2013 *Astrophys. Space Sci.* **347** 299
[18] Mehdipour S H and Keshavarz A 2012 *Europhys. Lett.* **98** 10002
[19] Bhar P, Rahaman F, Biswas R and Mondal U 2015 *Commun. Theor. Phys.* **64** 1
[20] Tejeiro J M and Larrañaga A 2011 *The Abraham Zelmanov Journal* **4** 28
[21] Rahaman F, Bhar P, Sharma R and Tiwari R K 2015 *Eur. Phys. J. C* **75** 107
[22] Tejeiro J M and Larrañaga A 2012 *Pramana J. Phys.* **78** 155
[23] Rahaman F, Kuhfittig P K F, Bhui B C, Rahaman M, Ray S and Mondal U F 2013 *Phys. Rev. D* **87** 084014
[24] Park M I 2009 *Phys. Rev. D* **80** 084026
[25] Myung Y S and Yoon M 2009 *Eur. Phys. J. C* **62** 405
[26] Liang J, Liu Y C and Zhu Q 2014 *Chin. Phys. C* **38** 025101
[27] Miao Y G and Xu Z M 2016 *Eur. Phys. J. C* **76** 217
[28] Tangherlini F R 1963 *Nuovo Cimento* **27** 636
[29] Daghigh R G, Kunstatter G, Ostapchuk D and Bagnulo V 2006 *Classical and Quantum Gravity* **23** 5101